ISSN 1063-7834, Physics of the Solid State, 2011, Vol. 53, No. 1, pp. 119–126. © Pleiades Publishing, Ltd., 2011.
Original Russian Text © V.I. Talanin, I.E. Talanin, 2011, published in Fizika Tverdogo Tela, 2011, Vol. 53, No. 1, pp. 114–120.

IMPURITY CENTERS

Kinetic Model of Growth and Coalescence of Oxygen and Carbon Precipitates during Cooling of As-Grown Silicon Crystals

V. I. Talanin* and I. E. Talanin

Classical Private University, ul. Zhukovskogo 70b, Zaporozh'e, 69002 Ukraine

** e-mail: v.i.talanin@mail.ru*

Received April 5, 2010; in final form, June 15, 2010

Abstract—A kinetic model of growth and coalescence of oxygen and carbon precipitates has been proposed. This model in combination with the kinetic model of the formation of oxygen and carbon precipitates represents a unified model of precipitation in as-grown dislocation-free silicon single crystals during their cooling in the temperature range from 1683 to 300 K. It has been demonstrated that the results of the calculations are in good agreement with the experimental data obtained from investigations of grown-in microdefects.

DOI: 10.1134/S1063783411010318

1. INTRODUCTION

A growing undoped silicon crystal can be represented as a multicomponent multiphase system in which the role of components is played by oxygen and carbon atoms, intrinsic interstitial silicon atoms, and vacancies, whereas oxygen and carbon precipitates and agglomerates of intrinsic point defects (vacancy microvoids and interstitial dislocation loops) should be treated as a new phase.

At present, there exist two models describing the process of precipitation during growth of dislocation-free silicon single crystals. The model of dynamics of point defects has assumed that precipitation of an impurity occurs at the last stage of the formation of an initial defect structure during cooling of the as-grown crystal at temperatures below 1123 K [1–4]. The diffusion model of the formation of grown-in microdefects has employed a combined simulation technique based on the solution of differential equations for small-sized clusters and the Fokker–Planck equation for large-sized clusters in the temperature range of cooling from 1683 to 1373 K [5, 6]. The calculations performed in terms of the model of dissociative diffusion, i.e., migration of impurities for small-sized nuclei, have demonstrated that the boundary of the reaction front of the formation of a complex (oxygen–vacancy and carbon–interstitial silicon atom) is located at a distance of $\sim 3 \times 10^{-4}$ mm from the crystallization front [5]. This distance represents a diffusion layer in which an excessive concentration of intrinsic point defects arises because of the absence of their recombination at high temperatures. In our recent papers [5, 6], it has been theoretically shown for the first time that the process of precipitation begins in the vicinity of the crystallization front due to the disappearance of excess intrinsic point defects on sinks whose role is played by oxygen and carbon impurities.

It should be noted that the stage of the formation of precipitates is described in the model of dynamics of point defects and in the diffusion model. At the same time, in the classical theory of nucleation and growth of new-phase particles, the process of precipitation in a crystal is treated as a first-order phase transition and the kinetics of this process is divided into three stages: the formation of new-phase nuclei, the growth of clusters, and the coalescence stage [7]. In this respect, the purpose of the present work was to formulate and solve the problem of description of the stages of the growth and coalescence of oxygen and carbon impurities during cooling of a silicon crystal in the course of the growth in the range from high temperatures to room temperature.

2. MATHEMATICAL MODEL OF GROWTH AND COALESCENCE OF GROWN-IN MICRODEFECTS (PRECIPITATES)

At the second stage of the precipitation process, clusters grow without a change in their number. This growth is accompanied by a considerable decrease in the degree of supersaturation of the solid solution. It is assumed that the growth kinetics of precipitates is described by the reversible scheme $A_iC + A \longleftrightarrow A_{i+1}C$, which corresponds to the growth of precipitates at the nucleation centers C with a concentration N_c that remains unchanged with time. The nucleation centers

attach and detach monomers, which is described by the system of equations [8]

$$\frac{dN_0}{dt} = -k_0 N N_0 + g_1 N_1,$$

$$\frac{dN_i}{dt} = -N_i(k_i N + g_i) + g_{i+1} N_{i+1} + k_{i-1} N N_{i-1}, \quad (1)$$

$$\frac{dN}{dt} = -N\sum_{i=0} k_i N_i + \sum_{i=1} g_i N_i,$$

where N_i is the volume-average concentration of nucleation centers that attach i particles, N is the monomer concentration, $k_i N$ is the rate of attachment of a monomer for a nucleation center, and g_i is the rate of detachment of a monomer for a nucleation center. At the initial instant of time, the system contains only monomers and nucleation centers. The growth of precipitates is limited by the monomer diffusion. The kinetic coefficients are given by the formula $k_i = 4\pi R_i D$, where R_i is the radius of attachment of a free particle by a cluster consisting of i particles and D is the diffusion coefficient of a free particle.

The system of equations (1) obeys the law of conservation of nucleation centers $N_c = \sum_{i=1} N_i(t)$ and the law of conservation of the total number of particles, including both monomers and particles involved in precipitates, i.e., $N(0) = N(t) + \sum_{i=1} iN_i$, where $N(0)$ is the monomer concentration at the initial instant of time. Therefore, the average number of particles at the nucleation centers can be represented in the form

$$i = \frac{\sum_{i=0} iN_i}{\sum_{i=0} N_i} = \frac{N(0) - N(t)}{N_c}. \quad (2)$$

For $i \gg 1$, the process is described using the Fokker–Planck equation [9]. In accordance with the principle of detailed balance $g(i) = k(i-1)N_E C_E(i-1)/C_E(i) \approx k(i)N_E$, the Fokker–Planck equation takes the form

$$\frac{\partial C(i,t)}{\partial t} = -(N(t) - N_E)\frac{\partial}{\partial i}(k(i)C(i,t)) + (N(t) + N_E)\frac{\partial^2}{2\partial i^2}(k(i)C(i,t)), \quad (3)$$

where N_E is the equilibrium concentration of monomers.

In the case of the diffusion-controlled precipitation, the mathematical expectation $i(t)$ can be described by the macroscopic equation [9] corresponding to expression (3):

$$\frac{di}{dt} = k_0(N - N_E)(i(t) + m)^{\alpha}, \quad (4)$$

where $k_0 = 4\pi R_i D$, m is the initial size of precipitates, and α is the parameter dependent on the cluster geometry.

Expressions (2) and (4) allow us to write the differential equation that describes the variation in the monomer concentration during the decomposition of the solid solution [8]:

$$\frac{dN(t)}{dt} = -k_0 N_c^{1-\alpha}(N(t) - N_E)(N(0) + mN_c - N(t))^{\alpha}. \quad (5)$$

The kinetics of decrease in the monomer concentration, which is determined from the numerical solutions to the system of initial equations (1), coincides with that obtained from expression (5), to within the error of numerical methods [8]. The solution of the system of initial equations (1) for real objects is nearly impossible due to the large dimension of the system of equations, whereas the solution of Eq. (5) presents no special problems [8].

The kinetics of decrease in the monomer concentration as a result of the decomposition of the solid solution at $m = 0$ can be written in the form

$$\frac{N(t) - N_E}{N(0) - N_E} = \exp\left\{-N_c[(1-\alpha)(N(0) - N_E)^{\alpha} k_0 t]^{\frac{1}{1-\alpha}}\right\}. \quad (6)$$

By numerically solving Eq. (5) simultaneously with Eq. (2), we can calculated the average radius of the precipitate at the growth stage:

$$R(t) = \sqrt[3]{\frac{3bi(t)}{4\pi}}. \quad (7)$$

At the third stage of the precipitation process, when the particles of the new phase are sufficiently large, the supersaturation is relatively low, new particles are not formed and the decisive role is played by the coalescence, which is accompanied by the dissolution of small-sized particles and the growth of large-sized particles. The condition providing for changeover to the coalescence stage is the ratio $u(t) = \frac{R(t)}{R_{cr}(t)} \approx 1$, where $R_{cr}(t)$ is the critical radius of the precipitate. Under this condition, the precipitate is in equilibrium with the solution $\left(\frac{dR}{dt} = 0\right)$. The precipitate grows at $R(t) > R_{cr}(t)$ and dissolves at $R(t) < R_{cr}(t)$. With time,

the critical radius $R_{cr}(t)$ increases and the number of particles per unit volume decreases [7, 10]. As was shown in [11], the solution of the system of equations describing this process is possible only in the case where the supersaturation of the solute tends to zero.

Slezov and Kukushkin [12] showed that the crystallization of single-component melts is accompanied by the formation of temperature fields and that the precipitates of the new phase interact with each other through generalized temperature fields. The asymptotic solution to the system of equations describing this process is similar to the solution of the equations describing the diffusion isothermal coalescence [11] and becomes possible when the supercooling of the melt $\Delta T = T_c - T_0$ tends to zero (where T_c and T_0 are the average and equilibrium temperatures of the crystal, respectively [12]).

Let us consider a solid solution that contains single-component spherical precipitates of a new phase with the initial size distribution function $f_0(R)$. The system containing the solid solution is thermally insulated and does not involve sources of a substance. Let the initial temperature and the initial concentration of the solid solution be $T_c(0)$ and $c_c(0)$, respectively. The solution is considered at the coalescence stage.

Since the system in which the solid solution decomposes is thermally insulated, the heat of the phase transition that releases in the course of the coalescence leads to an increase in the temperature of the entire system, which, in turn, leads to a change in the equilibrium concentration c_0 [12]. In this case, the supersaturation will tend to zero more rapidly than in the case of isothermal coalescence, because the increase in the temperature results in an increase in the equilibrium concentration c_0 [13]. This will lead to a decrease in the concentration gradient between the solution and the precipitation of the new phase, and, correspondingly, the growth rate of precipitates decreases. Consequently, the diffusion and thermal fields become self-consistent and the system of equations of the nonisothermal coalescence should involve both the mass balance equation and the heat balance equation. The system of equations describing the nonisothermal coalescence has the form [12]

$$\frac{\partial f(R,t)}{\partial t} + \frac{\partial}{\partial R}[f(R,t)dR/dt] = 0, \qquad f_0(R) = f(R,0), \tag{8}$$

$$Q(T_c) = c_c(t) + \chi\int_0^\infty f(R,t)R^3 dR, \tag{9}$$

$$T_c(t) = T_c(0) + \frac{L\chi}{c_p\rho_t}\int_0^\infty [f(R,t) - f_0(R)]R^3 dR, \tag{10}$$

where expression (8) is the equation of continuity in the space of sizes for the size distribution function of precipitates, expression (9) is the mass balance equation, expression (10) is the equation accounting for the amount of released heat, $f_0(R)$ is the initial size distribution function of precipitates, $T_c(0)$ is the initial temperature of the solid solution, $\chi = 4\pi/3v$, v is the volume per atom in the precipitates of the new phase, $Q(T_c)$ is the total amount of the material in the precipitates and the solution, $c_c(t)$ is the solute concentration in the solid solution, L is the heat of the phase transition per atom of the precipitated phase, c_p is the heat capacity at constant pressure per unit mass of the solid solution, and ρ_e is the density of the solid solution. The average temperature of the solid solution is a function of the amount of the material in the precipitates of the new phase; i.e., Eqs. (9) and (10) are related to each other.

In order for the system of equations (8)–(10) to be complete, it is necessary to find the dependence of the growth rate of precipitates dR/dt on the radius R:

$$\frac{dR}{dt} = -Dv\frac{\partial c}{\partial r}. \tag{11}$$

Here, D is the diffusion coefficient for the component forming the new phase; $\frac{\partial c}{\partial r}$ is the concentration gradient of atoms at the precipitate boundary, which will be determined from the quasi-steady-state (the supersaturation is relatively low) solution of the diffusion equation written in the spherical coordinates

$$\frac{\partial^2 c}{\partial r^2} + \frac{2}{r}\frac{\partial c}{\partial r} = 0 \tag{12}$$

with the boundary conditions [12]

$$c_{r\to\infty} = c_c(T_c), \quad c_{r=R} = c(R), \qquad D\frac{\partial c}{\partial r} = \beta v(c(R) - c_R), \tag{13}$$

where β is the specific boundary flux, which includes the rate of incorporation of the emission of atoms into the precipitate; c_R is the concentration of atoms in equilibrium with the precipitate of radius R; and $c(R)$ is the concentration at the surface of the precipitate of the new phase. In the case of nonisothermal coalescence, the concentrations c_c, $c(R)$, and c_R are functions of the temperature T_c. The equation for the

growth rate of a precipitate is obtained by solving Eq. (12) with the boundary conditions (13):

$$\frac{dR}{dt} = \frac{2\sigma D v^3 \beta c_0(T_c)}{kT_c(D+\beta v R)R^2}(R/R_k - 1), \quad (14)$$

where $c_0(T_c)$ is the equilibrium concentration of the solute at the temperature T_c and σ is the surface tension at the interface between the precipitate of the new phase and the solid solution. It follows from expression (14) that there are two possible processes limiting the growth rate of the precipitate [12].

(1) The diffusion processes for $D \ll \beta v R$:

$$\frac{dR}{dt} = \frac{2\sigma D v^2 c_0(T_c)}{kT_c R^2}(R/R_k - 1). \quad (15)$$

(2) The processes occurring at the precipitate boundary for $D \gg \beta v R$:

$$\frac{dR}{dt} = \frac{2\sigma D v^3 c_0(T_c)\beta}{kT_c R}(R/R_k - 1). \quad (16)$$

Equations (8)–(10) with either expression (15) or expression (16) form the complete system of equations that describe the process of nonisothermal decomposition of the solid solution at the stage of the coalescence. Slezov and Kukushkin [12] showed that, in closed systems in the absence of sources (sinks) of heat and matter, the dependences of the variations in the distribution functions for precipitates of the new phase over the sizes, their density, and the critical and average radii in the case of nonisothermal coalescence are identical to those observed in the case of isothermal coalescence [11]. Only the constants dependent on the temperature are changed. Equations (8)–(10), together with either expression (15) or expression (16), are solved using the method developed in [11]. In the general case, the size distribution function for precipitates has the following form:

$$f(R,t) = \frac{n(t)}{R_{cr}(t)}P(u), \qquad u = \frac{R(t)}{R_{cr}(t)}, \quad (17)$$

$$P(u) = \begin{cases} -\dfrac{16u\exp\left[\dfrac{3u}{u-2}\right]}{(u-2)^5}, & u < 2 \\ 0, & u > 2. \end{cases} \quad (18)$$

The average size of precipitates at the stage of the coalescence is proportional to the cube root of time [12]:

$$R_{av}(t) = \sqrt[3]{R_{cr}^3(t_0) + \frac{4D\beta t}{9}}, \quad (19)$$

where D is the diffusion coefficient of impurity atoms, $\beta = \left(\frac{\sigma\Omega}{kT}\right)N(0)$, $R_{cr}(t_0)$ is the initial critical radius, σ is the surface tension at the precipitate–solid solution interface, Ω is the atomic volume, and

$$n(t) = \frac{N_c}{t/t_0}. \quad (20)$$

Here, t_0 is the initial critical time and N_c is the initial concentration of precipitates.

3. EXPERIMENTAL RESULTS

The calculations were performed using the following parameters: $V_p = 4.302 \times 10^{-2}$ nm^3 (SiO_2), $V_p = 2.040 \times 10^{-2}$ nm^3 (SiC), $\sigma = 310$ erg/cm^2 (SiO_2), $\sigma = 1000$ erg/cm^2 (SiC), $\mu = 6.41 \times 10^{10}$ Pa, $\sigma = 0.30$, $\varepsilon = 0.15$ [12], $b = 0.25$ nm, $D_0 = 0.17\exp(-2.54\ \text{eV}/kT)$, $D_c = 1.9\exp(-3.1\ \text{eV}/kT)$, and $k = 8.6153 \times 10^{-5}$ eV/K.

The analysis was carried out under the assumption that precipitates grow at a fixed number of nucleation centers according to the diffusion mechanism of growth. The model corresponds to the precipitation uniform in the volume.

We performed four separate groups of calculations that simulated the processes of precipitation during the growth of crystals of large and small diameters with the use of the Czochralski method and floating zone melting. Calculations of the first group (I) were performed using the following parameters: the crystal growth rate was $V = 0.6$ mm/min, the axial temperature gradient was $G = 2.5$ K/mm, the oxygen concentration was $N(0) = 10^{18}$ cm^{-3}, and the carbon concentration was $N(0) = 10^{18}$ cm^{-3}. These conditions correspond to the growth of large-sized silicon single crystals with the use of the Czochralski method (CZ-Si). The corresponding parameters used in calculations of the second group (II) were as follows: the crystal growth rate was $V = 6$ mm/min, the axial temperature gradient was $G = 13$ K/mm, the oxygen concentration was $N(0) = 10^{18}$ cm^{-3}, and the carbon concentration was $N(0) = 10^{18}$ cm^{-3}. For calculations of the third group (III), we used the following parameters: the crystal growth rate was $V = 6$ mm/min, the axial temperature gradient was $G = 13$ K/mm, the oxygen concentration was $N(0) = 8 \times 10^{16}$ cm^{-3}, and the carbon concentration was $N(0) = 10^{16}$ cm^{-3}. The corresponding parameters used in calculations of the fourth group (IV) were

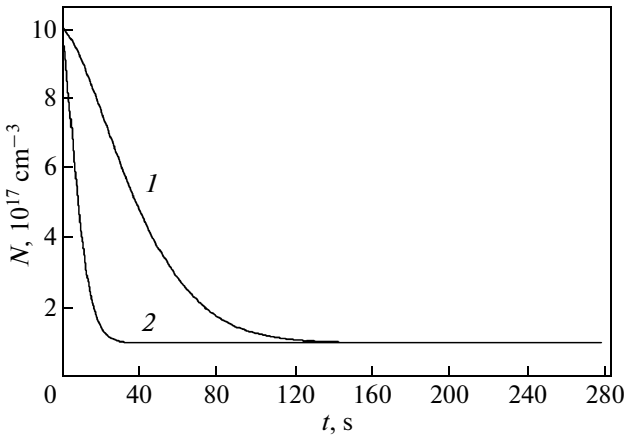

Fig. 1. Variation of the concentration of (*1*) oxygen and (*2*) carbon monomers during cooling of the CZ-Si crystal from the crystallization temperature.

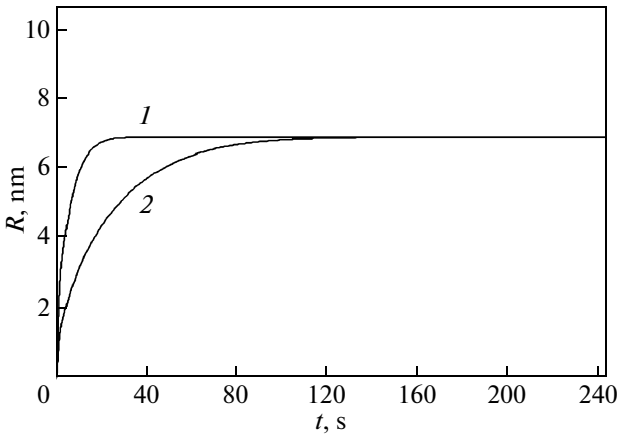

Fig. 2. Variation of the average size R of (*1*) oxygen and (*2*) carbon precipitates at the stage of the growth during cooling of the CZ-Si crystal from the crystallization temperature.

as follows: the crystal growth rate was $V = 6$ mm/min, the axial temperature gradient was $G = 13$ K/mm, the oxygen concentration was $N(0) = 4 \times 10^{15}$ cm^{-3}, and the carbon concentration was $N(0) = 4 \times 10^{15}$ cm^{-3}. Groups II–IV correspond to the conditions for growth of small-sized silicon single crystals with the use of floating zone melting (FZ-Si). For all four groups of calculations, we used $T = \dfrac{T_m^2}{T_m + VGt}$, where T_m is the melting temperature, $N(0) = 0.1N_E$ [8], $N_c = 10^{13}$ cm^{-3} [14], and $\alpha = 1/3$ [8].

The results of the calculations performed in groups I and II allow us to compare the processes of precipitation in the CZ-Si and FZ-Si crystals and to analyze them for almost maximum contents of the oxygen and carbon impurities. The kinetics of decrease in the concentrations of oxygen and carbon monomers in the CZ-Si crystals is illustrated in Fig. 1. The average size of precipitates is approximately equal to 14 nm (Fig. 2), and their initial concentration is determined from experiments on quenching of the crystals ($\sim 10^{12}$–10^{13} cm^{-3}) [14].

An analysis of the results obtained and the data taken from [5, 6] has demonstrated that the phase transition occurs according to the mechanism of nucleation and growth of a new phase so that these two processes are not separated in time and proceed in parallel.

An important parameter that characterizes the process of precipitation of impurities in silicon is the critical radius of precipitates [15]

$$R_{\rm cr}^{\rm O} = \frac{2\sigma u V_p}{kT\ln(S_{\rm O}S_i^{-\gamma_i}S_v^{\gamma_v}) - 6\mu\delta\varepsilon u V_p}, \qquad (21)$$

$$R_{\rm cr}^{\rm C} = \frac{2\sigma u V_p}{kT\ln(S_{\rm C}S_i^{\gamma_i}S_v^{-\gamma_v}) - 6\mu\delta\varepsilon u V_p}, \qquad (22)$$

where $S_{\rm O} = C_{\rm O}/C_{\rm O}^{\rm eg}$, $S_{\rm C} = C_{\rm C}/C_{\rm C}^{\rm eg}$, $S_i = C_i/C_i^{\rm eg}$, and $S_v = C_v/C_v^{\rm eg}$ are the supersaturations of the oxygen atoms, carbon atoms, intrinsic interstitial silicon atoms, and vacancies, respectively; σ is the density of the surface energy of the interface between the precipitate and the matrix; μ is the shear modulus of silicon; δ and ε are the linear and volume misfit strains of the precipitate and the matrix, respectively; γ_i and γ_v are the fractions of intrinsic interstitial silicon atoms and vacancies per impurity atom attached to the precipitate, respectively; V_p is the molecular volume of the precipitate; and $u = (1 + \gamma_i x + \gamma_v x)^{-1}\left(\dfrac{1+\varepsilon}{1+\delta}\right)^3$.

The condition providing changeover to the stage of the coalescence is written in the form $R(t) \approx R_{\rm cr}(t)$, which is satisfied at the temperature $T \approx 1423$ K. Taking into account the computational errors, this temperature for large-sized crystals corresponds to the initial point of the range of the formation of vacancy microvoids (at $V = 0.6$ mm/min). In this range, all impurities are bound and there arises a supersaturation with respect to vacancies, which is removed as a result of the formation of vacancy microvoids. With a change in the thermal conditions of the growth (for example, at $V = 0.3$ mm/min [3]), there arises a supersaturation with respect to interstitial silicon atoms, which leads to the formation of interstitial dislocation loops. In this case, the condition $R(t) = R_{\rm cr}(t)$ is satisfied at $T \approx 1418$ K. Consequently, the stage of the coalescence in large-sized silicon single crystals begins at tempera-

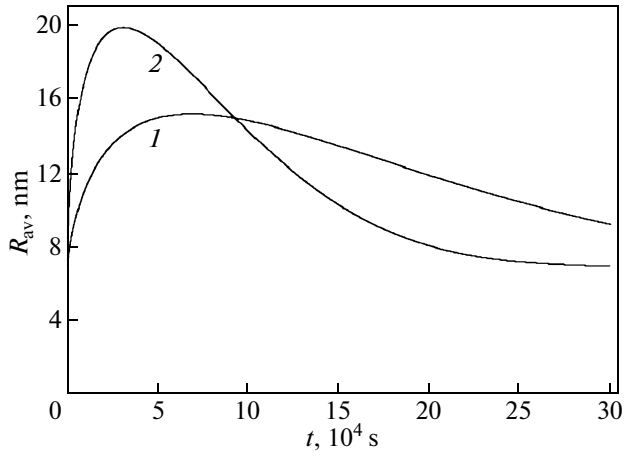

Fig. 3. Variation of the average size R_{av} of (*1*) oxygen and (*2*) carbon precipitates at the stage of the coalescence during cooling of the CZ-Si crystals in the temperature range from 1423 to 300 K.

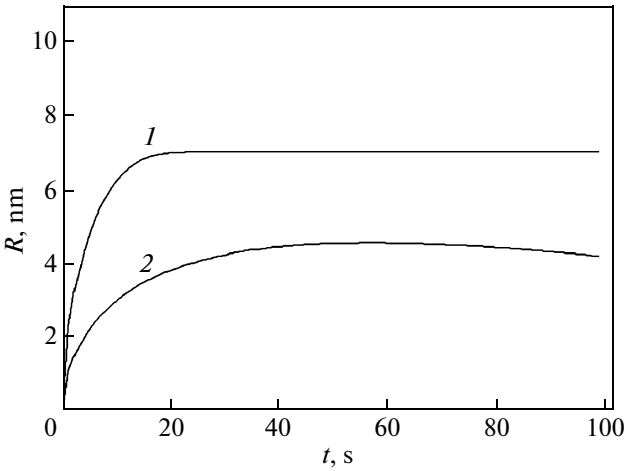

Fig. 4. Variation of the average size R of (*1*) oxygen and (*2*) carbon precipitates during cooling of the FZ-Si crystal (II) from the crystallization temperature.

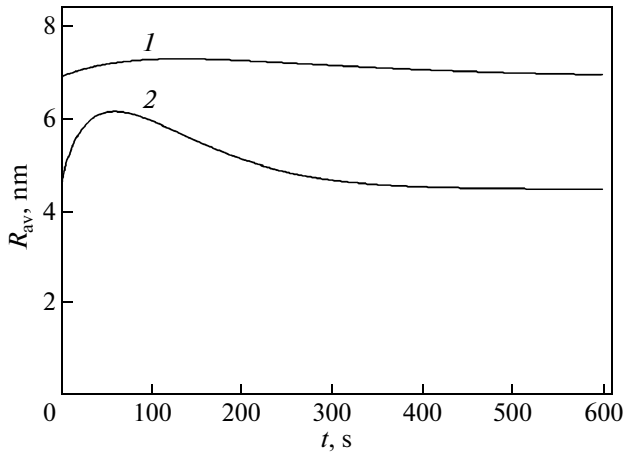

Fig. 5. Variation of the average size R_{av} of (*1*) oxygen and (*2*) carbon precipitates during cooling of the FZ-Si crystals (II) in the temperature range from 1423 to 300 K.

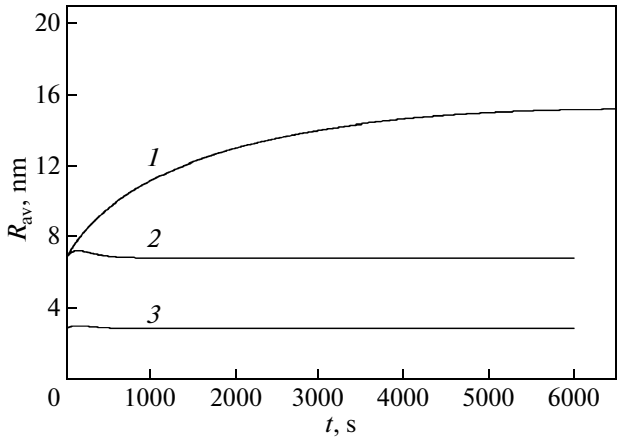

Fig. 6. Variation of the average size R_{av} of oxygen precipitates at the stage of the coalescence for crystals of groups (*1*) I, (*2*) II, and (*3*) III.

tures close to the temperatures of the formation of clusters of intrinsic point defects (depending on the thermal growth conditions, these are vacancy microvoids or interstitial dislocation loops).

Figure 3 shows the variation of the average size of oxygen and carbon precipitates at the stage of the coalescence in the temperature range of cooling from 1423 to 300 K. At this stage of the calculations, we used the temperature dependences of the diffusion coefficients for oxygen $D_O = 2.16 \times 10^{-6}\exp(-1.55/kT)$ cm^2/s [16] and carbon $D_C = 1.3\exp(-3.3/kT)$ cm^2/s [17].

The calculations in group II showed that the change in thermal conditions of the growth leads to a decrease in the average radius of precipitates $R(t)$ in the FZ-Si crystals as compared to the CZ-Si crystals in group I (Fig. 4) at the stage of the growth of precipitates, as well as to the corresponding decrease in the precipitate sizes at the stage of the coalescence (Fig. 5).

The results of the calculations of the variation in the average size of oxygen precipitates at the stage of the coalescence for crystals of groups I–III are presented in Fig. 6, and the corresponding results of the calculations of the variation in the average size of carbon precipitates at the stage of the coalescence for crystals of groups I–III are presented in Fig. 7.

The simultaneous nucleation and growth of particles of the new phase (oxygen and carbon precipitates) during cooling of as-grown silicon crystals leads to a strong interplay between the processes of evolution of these two subsystems of grown-in microdefects. The

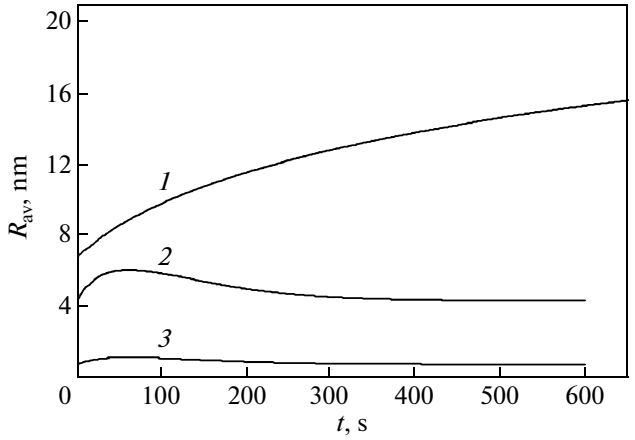

Fig. 7. Variation of the average size R_{av} of carbon precipitates at the stage of the coalescence for crystals of groups (*1*) I, (*2*) II, and (*3*) III.

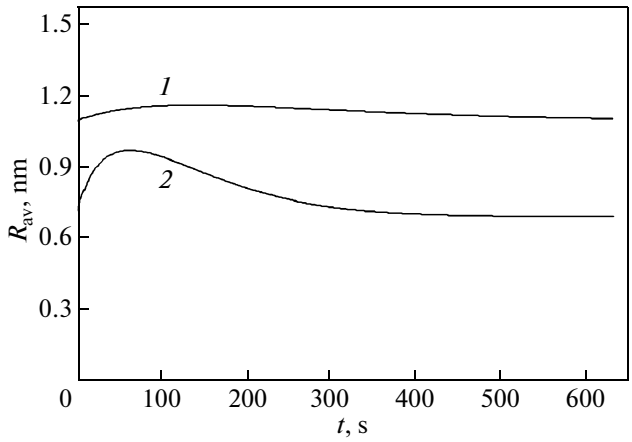

Fig. 8. Variation of the average size R_{av} of (*1*) oxygen and (*2*) carbon precipitates at the stage of the coalescence for crystals of group IV.

absorption of vacancies by growing oxygen precipitates results in the emission of silicon atoms in interstitial sites. In turn, the intrinsic interstitial silicon atoms interact with growing carbon precipitates, which, in the course of their growth, supply vacancies for growing oxygen precipitates. This interplay between the processes leads to an accelerated changeover of the subsystems of oxygen and carbon precipitates to the stage of the coalescence as compared to the independent evolution of these two subsystems.

Although the concentrations of oxygen and carbon in crystals of groups I and II are identical, the change in the thermal conditions for the growth of small-sized FZ-Si single crystals (high growth rates and axial temperature gradients) leads to the fact that the stage of the coalescence begins far in advance (at $T \approx T_m - 20$ K).

The results of the calculations performed for crystals of groups III and IV have attracted the particular attention. It is worth noting that the calculations carried out for crystals of groups I and II are of theoretical interest for the case of limiting concentrations of oxygen and carbon under different thermal growth conditions (different methods used for growing crystals and different crystal diameters), whereas for real crystals of groups III and IV, there are experimental results of the investigations performed using transmission electron microscopy [14].

The results of theoretical calculations have demonstrated that a decrease in the concentrations of oxygen and carbon in crystals of groups III and IV leads to a further decrease in the time of occurrence of the growth stage of precipitates (for example, the stage of the coalescence for crystals of group IV begins at $T = T_m - 5$ K). Consequently, the change in thermal conditions of crystal growth (in particular, an increase in the growth rate and in the axial temperature gradient in the crystal) substantially affects the stage of the growth of precipitates. In turn, the decrease in the time of occurrence of the growth stage of precipitates is associated, to a lesser extent, with the decrease in the concentration of impurities in crystals. Eventually, these factors are responsible for the decrease in the average size of the precipitates (Figs. 6–8).

Previously, detailed electron microscopy investigations have established that the oxygen and carbon precipitates (grown-in *D*-microdefects under the given thermal growth conditions) have sizes in the range 3–10 nm and that their concentration is approximately equal to 10^{13} cm^{-3} [14]. A decrease in the crystal growth rate results in an increase in the defect size [14, 18]. An analysis of the results of the computer simulation has demonstrated that the final size of precipitates lies in the range 2.7–6.5 nm for crystals of group III and in the range 2.0–5.5 nm for crystals of group IV, which in very good agreement with the experimental data [18].

4. CONCLUSIONS

Thus, the proposed kinetic model of decomposition of solid solutions of oxygen and carbon impurities not only allows one to simulate the processes of precipitation during cooling of the as-grown silicon crystal to a temperature of 300 K but also adequately describes the available experimental data on the oxygen and carbon precipitation. The kinetic model of growth and coalescence of oxygen and carbon precipitates in combination with the kinetic models describing their formation [5, 6] represents a unified model of the process of precipitation in dislocation-free silicon single crystals. In the future, the mathematical apparatus of this model will make it possible to take into account and analyze interactions of intrinsic point

defects not only with oxygen and carbon background impurities but also with other impurities (for example, transition metals, nitrogen, hydrogen, etc.), as well as interactions of the impurity–impurity type.

In turn, the unified model of precipitation, together with the kinetic models of the formation and growth of interstitial dislocation loops and vacancy microvoids [19, 20], provides a mathematical apparatus for an adequate theoretical description of the processes of formation and transformation of grown-in microdefects in dislocation-free silicon single crystals of any diameter that are prepared using the floating zone melting and Czochralski methods. The use of this approach is based on the physical model founded on the theoretically and experimentally established fact that no recombination of intrinsic point defects occurs during cooling of crystals in the course of their growth at high temperatures [14, 21].

REFERENCES

1. V. V. Voronkov, J. Cryst. Growth **59**, 625 (1982).
2. T. Sinno and R. A. Brown, J. Electrochem. Soc. **146**, 2300 (1999).
3. M. S. Kulkarni, V. V. Voronkov, and R. Falster, J. Electrochem. Soc. **151**, G663 (2004).
4. A. I. Prostomolotov and N. A. Verezub, Solid State Phenom. **131–133**, 283 (2008).
5. V. I. Talanin, I. E. Talanin, and A. A. Voronin, Can. J. Phys. **85**, 1459 (2007).
6. V. I. Talanin and I. E. Talanin, Fiz. Tverd. Tela (St. Petersburg) **52** (10), 1925 (2010) [Phys. Solid State **52** (10), 2063 (2010)].
7. L. D. Landau and E. M. Lifshitz, *Course of Theoretical Physics*, Vol. 10: E. M. Lifshitz and L. P. Pitaevskii, *Physical Kinetics* (Nauka, Moscow, 1979; Butterworth–Heinemann, Oxford, 1981).
8. S. V. Bulyarskii, V. V. Svetukhin, and O. V. Prikhod'ko, Fiz. Tekh. Poluprovodn. (St. Petersburg) **33** (11), 1281 (1999) [Semiconductors **33** (11), 1157 (1999)].
9. N. G. Van Kampen, *Stochastic Processes in Physics and Chemistry* (Vysshaya Shkola, Moscow, 1990; Elsevier, Amsterdam, 1992).
10. V. V. Slezov and V. V. Sagalovich, Usp. Fiz. Nauk **151** (1), 67 (1987) [Sov. Phys.—Usp. **30** (1), 23 (1987)].
11. I. M. Lifshitz and V. V. Slezov, Zh. Eksp. Teor. Fiz. **35**, 479 (1958) [Sov. Phys. JETP *8*, 331 (1958)].
12. V. V. Slezov and S. A. Kukushkin, Fiz. Tverd. Tela (Leningrad) **29** (6), 1812 (1987) [Sov. Phys. Solid State **29** (6), 1041 (1987)].
13. L. D. Landau and E. M. Lifshitz, *Course of Theoretical Physics*, Vol. 5: *Statistical Physics: Part 1* (Nauka, Moscow, 1976; Butterworth–Heinemann, Oxford, 1980).
14. V. I. Talanin and I. E. Talanin, in *New Research of Semiconductors*, Ed. by T. B. Elliot (Nova Science, New York, 2006), p. 31.
15. J. Vanhellemont, J. Appl. Phys. **78**, 4297 (1995).
16. Z. Wang, *Modeling Microdefects Formation in Crystalline Silicon: The Roles of Point Defects and Oxygen* (Massachusetts Institute of Technology, Cambridge, Massachusetts, United States, 2002).
17. S. Henke, B. Stritzker, and B. Rauschenbach, J. Appl. Phys. **78**, 2070 (1995).
18. A. A. Sitnikova, L. M. Sorokin, I. E. Talanin, E. G. Sheikhet, and E. S. Falkevich, Phys. Status Solidi A **90**, K31 (1985).
19. V. I. Talanin and I. E. Talanin, Kristallografiya **55** (4), 675 (2010) [Crystallogr. Rep. **55** (4), 632 (2010)].
20. V. I. Talanin and I. E. Talanin, Fiz. Tverd. Tela (St. Petersburg) **52** (9), 1751 (2010) [Phys. Solid State **52** (9), 1880 (2010)].
21. V. I. Talanin and I. E. Talanin, Fiz. Tverd. Tela (St. Petersburg) **49** (3), 450 (2007) [Phys. Solid State **49** (3), 467 (2007)].

Translated by O. Borovik-Romanova